ADAM10 Inhibition of Human CD30 Shedding Increases Specificity of Targeted Immunotherapy *In vitro*

Dennis A. Eichenauer,[1] Vijaya Lakshmi Simhadri,[1] Elke Pogge von Strandmann,[1]
Andreas Ludwig,[3] Vance Matthews,[4] Katrin S. Reiners,[1] Bastian von Tresckow,[1,2]
Paul Saftig,[3] Stefan Rose-John,[2] Andreas Engert,[1] and Hinrich P. Hansen[1]

[1]Department of Internal Medicine I and [2]Center for Molecular Medicine, University Hospital Cologne, Cologne, Germany; [3]Department of Biochemistry, University of Kiel, Kiel, Germany; and [4]Ludwig Institute for Cancer Research, PO Royal Melbourne Hospital, Victoria, Melbourne, Australia

Abstract

CD30 is a transmembrane protein selectively overexpressed on many human lymphoma cells and therefore an interesting target for antibody-based immunotherapy. However, binding of therapeutic antibodies stimulates a juxtamembrane cleavage of CD30 leading to a loss of target antigen and an enhanced release of the soluble ectodomain of CD30 (sCD30). Here, we show that sCD30 binds to CD30 ligand (CD153)–expressing non-target cells. Because antibodies bind to sCD30, this results in unwanted antibody binding to these cells via sCD30 bridging. To overcome shedding-dependent damage of normal cells in CD30-specific immunotherapy, we analyzed the mechanism involved in the release. Shedding of CD30 can be enhanced by protein kinase C (PKC) activation, implicating the disintegrin metalloproteinase ADAM17 but not free cytoplasmic calcium. However, antibody-induced CD30 shedding is calcium dependent and PKC independent. This shedding involved the related metalloproteinase ADAM10 as shown by the use of the preferential ADAM10 inhibitor GI254023X and by an ADAM10-deficient cell line generated from embryonically lethal ADAM10$^{-/-}$ mouse. In coculture experiments, the antibody-induced transfer of sCD30 from the human Hodgkin's lymphoma cell line L540 to the CD30-negative but CD153-expressing human mast cell line HMC-1 was inhibited by GI254023X. These findings suggest that selective metalloproteinase inhibitors blocking antibody-induced shedding of target antigens could be of therapeutic value to increase the specificity and reduce side effects of immunotherapy with monoclonal antibodies. [Cancer Res 2007;67(1):332–8]

Introduction

A common feature of Hodgkin's lymphoma and large cell anaplastic lymphoma is the strong surface expression of CD30, a type I transmembrane receptor (1). Healthy donors express CD30 exclusively on very few cells, predominantly on activated lymphocytes. In contrast, the cognate ligand (CD153), a membrane-anchored type II glycoprotein, is expressed on the cell surface of many different cell types, including resting B cells, activated T cells, mast cells, monocytes, and granulocytes (2, 3).

Due to its selective expression, CD30 is generally well suited for targeted immunotherapy of CD30-positive lymphomas. Although antibody-based reagents against CD30 showed impressive anti-tumor activity in experimental Hodgkin's lymphoma models, early clinical trials suffered from dose-limiting toxicities (4). A problem that appeared was the formation of complexes containing the therapeutic antibody and the soluble ectodomain of CD30 (sCD30). sCD30 is generated by proteolytic cleavage of CD30 (5). The release of extracellular domains, also referred to as ectodomain shedding, is a general process regulating the function of membrane proteins (6). In most cases, shedding is catalyzed by metalloproteinases. The tumor necrosis factor-α (TNF-α)–converting enzyme, also known as a disintegrin and metalloproteinase 17 (ADAM17), is the metalloproteinase responsible for the ectodomain release of many membrane proteins, including CD30 (7, 8). A structurally related proteinase (ADAM10) is also implicated in certain shedding processes, such as the non-amyloidogenic processing of Alzheimer's amyloid precursor protein (APP; ref. 9) or the cleavage of N-cadherin and E-cadherin (10, 11).

Many studies distinguish between the mechanisms underlying the constitutive shedding of unstimulated cells and the release from stimulated cells. Classic shedding stimulation is initiated by the protein kinase C (PKC) activator phorbol 12-myristate-13-acetate (PMA), and there is evidence for an implication of ADAM17 (12). In some cases, including CD30, membrane protein shedding is also stimulated by antibody binding (6, 13). As the release of soluble antigen from tumor cells has far-reaching implications for targeted immunotherapy, our group has investigated the use of metalloproteinase inhibitors to block the release of the target antigen (14). In a mouse model, we showed that an anti-CD30 immunotoxin was only effective against human Hodgkin's lymphoma tumors when concomitantly used with the broad-spectrum hydroxamic acid–based metalloproteinase inhibitor BB-3644 (15). Such nonselective inhibitors block many different metalloproteinases, including essential matrix and disintegrin metalloproteinases. They have been used in clinical studies, and the broad specificity resulted in more unspecific toxicity than antitumor effects (16). Thus, more selective inhibitors are desirable for clinical use.

Here, we analyze the mechanism of antibody-stimulated release of sCD30. We found that antibody-induced CD30 shedding was not catalyzed by the previously described ADAM17 but instead by ADAM10. Moreover, we show that immunocompetitive sCD30 not only resided in a soluble form in the pericellular environment but also specifically bound to membrane-anchored CD30 ligand (CD153) on non-target cells where it generated novel targeting sites. Application of an ADAM10-selective metalloproteinase inhibitor significantly reduced this mistargeting.

Materials and Methods

Cells and reagents. We used the CD30$^+$/CD153$^-$ cell lines L540 (Hodgkin's lymphoma) and Karpas 299 (large cell anaplastic lymphoma) and the CD30$^-$/CD153$^+$ cell line DG75 (Burkitt lymphoma) and the CD30$^-$/CD153$^-$ cell line Reh (acute lymphoblastic leukemia). In addition, we used the mast cell line HMC-1, which was kindly provided by Dr. J. Butterfield (Mayo Clinic, Rochester, MN); the ADAM17-targeted mouse fibroblast cells, which were received from Dr. R. Black (Amgen Incorporated, Seattle, WA); and the ADAM10 ($^{-/-}$) cells, which were a gift of Dr. D. Hartmann (Center for Human Genetics, Leuven, Belgium). The hydroxamate inhibitor BB-3644 [2S-(2,2-dimethyl-propyl)-N^1-[2,2-dimethyl-1-(pyridin-2S-ylcarbamoyl)-propyl]-N^4-hydroxy-3R-methoxy-succinamide] was from British Biotech Pharmaceuticals Ltd. (Oxford, United Kingdom). GW280264 [(2R,3S)-3-(formylhydroxyamino)-2-(2-methyl-1-propyl) hexanoic acid (1S)-5-(benzyloxycarbamoyl-amino-1-(1,3-thiazol-2-ylcarbamoyl)-1-pentyl amide)] and GI254023X [(2R,3S)-3-(formyl-hydroxyamino)-2-(3-phenyl-1-propyl) butanoic acid [(1S)-2,2-dimetyl-1-methylcarbamoyl-1-propyl] amide] were from GlaxoSmithKline (Stevenage, United Kingdom). Recombinant ADAM10 was from Merck Biosciences (Schwalbach, Germany), and ADAM17 was from R&D Systems (Wiesbaden, Germany).

Plasmids. Construction of recombinant CD30Fc. The CD30Fc fusion protein containing the Fc portion of human IgG1 and the truncated ectodomain of human CD30 (deletion between ^{89}Arg and ^{156}Arg) was constructed by PCR using the CD30 cDNA clone (17), the *Hind*III forward primer 5′-GCGAGAAGCTTATGCGCGTCCTCCTCGCCGCG-3′, and the *Bam*HI reverse primer 5′-AGTGACGGATCCACTTACCTGTTGATGAGTATT-TATGATAACAAAGT-3′. The PCR product was cloned into the pIg fusion expression vector (Novagen, Madison, WI).

Construction and expression of CD153-glutathione *S*-transferase fusion protein. The ectodomain of CD153 was amplified by PCR using cDNA from DG75 cells and the primers 5′-CGACAGGATCCCCGTTCAGAGGACG-GACTCCATTCCCAAC-3′ and 5′-CAAGAGAATTCGTTCAGTCTGAAT-TACTGTATAAGAAGATGGAC-3′. After *Bam*HI and *Eco*RI restriction digest, the PCR product was cloned into the glutathione *S*-transferase (GST) expression vector (pGEX-3X, Amersham Pharmacia Biotech, Freiburg, Germany). BL21 cells (DE3) were transformed and induced for 5 h by isopropyl-L-thio-β-D-galactopyranoside (0.5 mmol/L). The bacterial pellet was suspended in 20 mmol/L Tris-HCl (pH 8) containing 150 mmol/L NaCl, 1 mmol/L EDTA, 5 mmol/L β-mercaptoethanol, 1% Triton X-100, and complete protease inhibitor cocktail (Roche Diagnostics, Mannheim, Germany). Lysozyme (0.5 mg/mL) was added to the suspension before sonication on ice (3×, 15 s). After centrifugation for 40 min at 35,000 × g and 4°C, the recombinant protein was extracted from the cell lysate by incubation with glutathione-conjugated agarose beads (GSH-agarose; Amersham Pharmacia Biotech). The beads were washed with lysis buffer without Triton X-100 and stored in 50 mmol/L Tris-HCl (pH 8).

Transfection. Cells were transfected as described previously (17). Transfection with cDNA for enhanced green fluorescence protein (Clontech, Palo Alto, CA) was used to monitor the transfection efficiency.

Production and purification of sCD30. 293T cells were transfected with CD30Fc or wild-type CD30 cDNA. After 48 h of incubation, CD30Fc or sCD30 was purified from the supernatants using Protein A Sepharose CL-4B beads (Amersham Pharmacia Biotech) or an anti-CD30 affinity matrix, respectively. In the latter, Ki-1 antibody was covalently linked to the matrix of a HiTrap NHS-activated HP column following the instructions of the manufacturer (Amersham Pharmacia Biotech). The eluted proteins were

Figure 1. Antibody-induced CD30 shedding is calcium dependent and PKC independent. *A,* stimulation of CD30 shedding. Karpas 299 cells (5 × 10^5 per mL) were stimulated with Ki-1, PMA, or calcium ionophore (*Cal*) for different periods of time as indicated. sCD30 was determined in cell-free supernatants. *Points,* mean for three independent experiments (U/mL); *bars,* SE. *B,* shedding inhibition. Karpas 299 cells were stimulated for 40 min with Ki-1 (3 μg/mL), PMA (30 ng/mL), or calcium ionophore (1 μmol/L). Stimulation was done in the presence or absence of BB-3644 (*BB*; 2 μmol/L), EGTA (*EG*; 3 mmol/L), or staurosporine (*ST*; 20 nmol/L). sCD30 was determined in cell-free supernatants. *Columns,* mean for at least three independent experiments (U/mL); *bars,* SE. *C,* induction of Ca^{2+} flux [(Ca^{2+})$_i$] in FLUO-3/AM–loaded Karpas 299 cells. Cells were stimulated with immobilized Ki-1 (3 μg/mL), PMA (30 ng/mL), or calcium ionophore A23187 (1 μmol/L), and fluorescence was determined by flow cytometry.
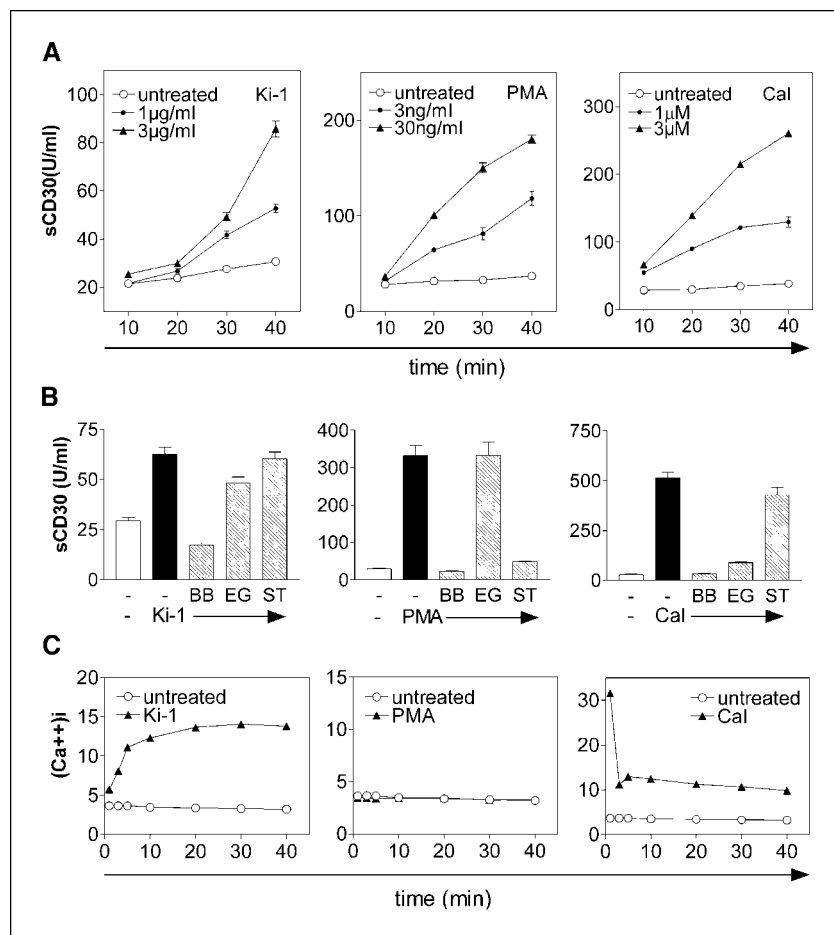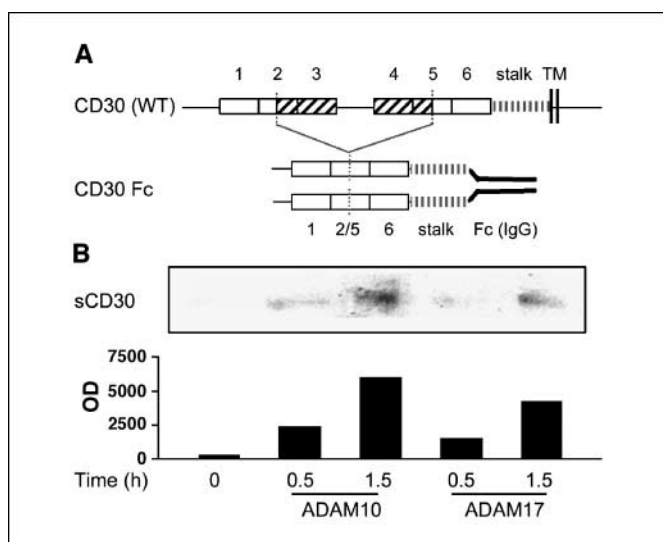
Figure 2. CD30 is cleaved by recombinant ADAM10. *A,* a truncated sCD30Fc protein was constructed. *B,* the protein (1 µg per lane) was treated with recombinant ADAM10 (70 ng) and ADAM17 (70 ng) for 30 or 90 min. CD30 was determined by Western blotting using a mixture of peroxidase-labeled Ki-2 and Ki-4 antibody. The quantity of the sCD30 bands was evaluated by density scan.

concentrated using Vivaspin concentrators (Vivascience, Hannover, Germany) and adjusted to 100,000 units/mL in PBS. The concentration was determined by sCD30 ELISA using Ki-2 as capture antibody and Ki-3 as detection antibody.

Determination of sCD30. The test was done as described previously (18).

Determination of calcium flux. Karpas 299 cells were suspended (10^7 per mL) in HBSS containing 5% FCS, 20 µmol/L Fluo 3-AM (Sigma, Taufkirchen, Germany), and 5 µL Pluronic F127 (25% in DMSO; Sigma). After 1 h of incubation at room temperature, cells were washed thrice with HBSS containing 5% FCS. Subsequent cell treatment was done at room temperature. The fluorescence was determined by FACScan flow cytometry.

Statistical analysis. The statistical significance was determined using the unpaired *t* test.

Results

Antibody-induced CD30 shedding is calcium dependent and PKC independent. First, we investigated the release of sCD30 from Karpas 299 cells. All agents, including PMA, the calcium ionophore A23187, and the anti-CD30 antibody Ki-1, stimulated the release of sCD30 in a time- and dose-dependent manner (Fig. 1*A*). The release was dependent on metalloproteinases because shedding was blocked by the broad-spectrum metalloproteinase inhibitor BB-3644 (Fig. 1*B*). However, more selective inhibitors indicate differences in the shedding mechanism. The PKC-selective inhibitor staurosporine, an inhibitor of the PMA-stimulated sCD30 release, failed to inhibit the antibody or ionophore effect. On the other hand, EGTA, a calcium-selective chelator, significantly inhibited the antibody or calcium ionophore–induced sCD30 release (both $P < 0.0001$, $n = 6$) but not the PMA effect ($P = 0.2597$, $n = 6$). This inhibition profile suggests a role of calcium in antibody but not in PMA-induced CD30 shedding. EGTA inhibition was weaker after antibody stimulation in comparison with that of A23187 treatment. This might be explained by the partially different source of calcium. Although ionophore primarily functions through calcium influx, effectively inhibited by cell membrane–impermeable EGTA, the cell signaling–induced increase in calcium is predominantly recruited from intracellular stores, not chelated by EGTA. In line with this

finding, the addition of Ki-1 and ionophore, but not PMA, caused an increase of cytoplasmic calcium levels in Karpas 299 cells (Fig. 1*C*). This suggests two different shedding pathways for CD30: one that is dependent on calcium but not on PKC, and another one that is dependent on PKC but not on calcium.

Evidence for a role of ADAM10 in antibody-induced CD30 shedding. Because the mechanism of antibody-stimulated CD30 shedding seems to be different from the PMA-stimulated shedding, we evaluated the responsible releasing enzymes. ADAM10 is of particular interest, as the ADAM10-dependent cleavage of CD44 is also associated with elevated cytoplasmic calcium levels (19). We initially compared the potency of recombinant ADAM10 and ADAM17 to cleave a soluble artificial substrate, containing the metalloproteinase-sensitive CD30 stalk domain flanked by a truncated ectodomain of CD30 and the Fc fragment of human IgG1 (Fig. 2*A*). Both ADAM10 (70 µg/mL) and ADAM17 (70 µg/mL) catalyzed the release of the 35-kDa ectodomain of the recombinant CD30 construct at 37°C in a time-dependent manner (Fig. 2*B*). The construct alone showed no decomposition within 24 h of incubation (data not shown). Thus, ADAM10 showed CD30 sheddase activity that was marginally greater compared with ADAM17, the known CD30 sheddase.

To investigate the role of ADAM10 in lymphoma cell culture, we used an ADAM10-selective inhibitor. This hydroxamic acid–based compound (GI254023X) inhibits ADAM10 >100 times more potently than ADAM17 (20). GI254023X (2 µmol/L) blocked antibody and calcium ionophore–induced shedding (Fig. 3*A* and *B*). Moreover, it partially inhibited constitutive CD30 shedding (Fig. 3*C*) but did not influence the PMA effect (Fig. 3*D*). Because the broad-spectrum hydroxamate inhibitors BB-3644 and GW280264X, at the same concentration, completely blocked all shedding stimulations in Karpas 299 lymphoma cells, the selective inhibition by GI254023X suggests a role of ADAM10 in anti-CD30 antibody and calcium ionophore–induced CD30 shedding.
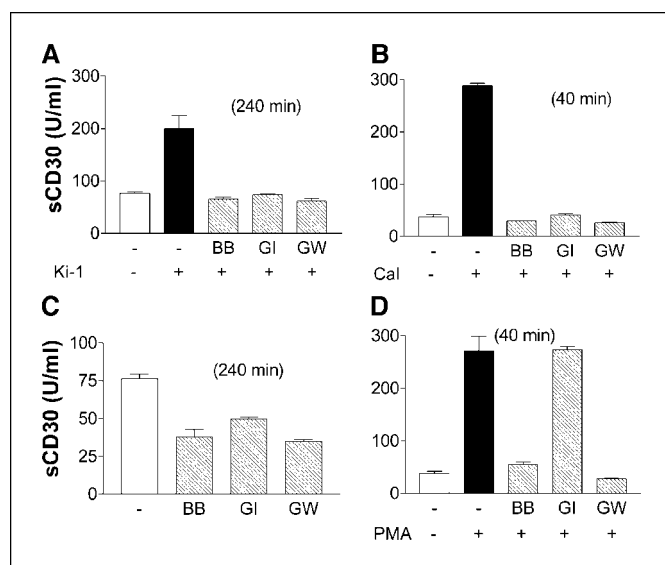
Figure 3. Selective inhibition of antibody-stimulated CD30 shedding. Karpas 299 cells were stimulated with Ki-1 (3 µg/mL; *A*), calcium ionophore (1 µmol/L; *B*), PMA (30 ng/mL; *D*), or not stimulated (*C*) in the presence or absence of the metalloproteinase inhibitors BB-3644 (*BB*), GI254023X (*GI*), or GW280264X (*GW*). Each inhibitor was used at a concentration of 2 µmol/L. sCD30 was determined in cell-free supernatants. *Columns,* mean for three independent experiments (U/mL); *bars,* SE.

To confirm the ADAM10 implication in CD30 shedding, we evaluated the release of sCD30 from ADAM10-deficient (ADAM10$^{-/-}$) murine fibroblasts (21, 22) with two different experimental readouts. First, cells were transfected with human CD30 cDNA and radiolabeled with a mixture of [^{35}S]methionine and [^{35}S]cysteine. The cells were then stimulated with Ki-1 antibody or PMA. sCD30 was isolated from cell supernatants by anti-CD30 immunoprecipitation. As shown in Fig. 4A, there is a constitutive liberation of the 90-kDa sCD30 from ADAM10$^{-/-}$ cells. This release was enhanced by PMA ($\times$1.3) but not by Ki-1 ($\times$0.8), indicating that antibody-stimulated CD30 shedding is dependent of ADAM10.

Then, a CD30-specific ELISA was used to compare the sCD30 release from ADAM10- or ADAM17-defective cells (Fig. 4B and C). Ki-1, which augments CD30 shedding in Karpas 299 cells, also stimulated the sCD30 release in ADAM17-defective cells ($\times$1.81, $P < 0.0001$, $n = 4$). However, in ADAM10-defective cells, the antibody rather caused a mild inhibition ($\times$0.85, $P < 0.0001$, $n = 6$; Fig. 4B), confirming a dominating role of ADAM10 in antibody-induced CD30 shedding. PMA, a known stimulator of ADAM17-dependent shedding (7), showed the reverse shedding pattern. This activator enhanced the sCD30 release in ADAM10-defective cells but caused no shedding stimulation in ADAM17-defective cells, rather a reduction ($\times$0.85, $P = 0.0002$, $n = 4$). Thus, the data further suggest that there are two different CD30-releasing enzymes: ADAM17, responsible for PMA-induced shedding and ADAM10, responsible for antibody-induced shedding. There is a constitutive release of CD30 found in ADAM10-defective and in ADAM17-defective cells, leading to the conclusion that both enzymes participate.

GI254023X was tested in this knockout setting to confirm its selectivity towards ADAM10 (i.e., inhibition of ADAM10 and non-inhibition of ADAM17). Indeed, it is remarkable that GI254023X at 2 μmol/L showed minor shedding inhibition in ADAM10-defective cells (Fig. 4A and B) but was blocking in ADAM10-expressing but ADAM17-defective fibroblasts (Fig. 4C). Hence, our study shows that GI254023X is a feasible tool to distinguish between ADAM10-defective and ADAM17-catalyzed CD30 shedding.

sCD30 bridges binding of anti-CD30 antibody to CD30 ligand-expressing cells. To determine the role of CD30 shedding in tumor cell targeting, we incubated CD30$^+$ targeting cells or CD30$^-$ non-targeting cells with sCD30 before staining with FITC-labeled Ki-1 antibody. As shown by flow cytometry, sCD30 (3,000 units/mL) strongly inhibited the binding of Ki-1 antibody to CD30$^+$ Karpas 299 cells (Fig. 5B). For the CD30$^-$/CD153$^+$ cell lines DG75 and HMC-1, we found the opposite effect. Although generally unable to bind the Ki-1 antibody, sCD30 communicated this binding. The effect was weak and correlated with the expression of CD153 on the cells (Fig. 5A), leading to the suggestion that the anti-CD30 antibody binds to CD153 using sCD30 as a linker. As a control, the CD30$^-$/CD153$^-$ cell line Reh did not bind the antibodies tested.

CD30$^+$ cells aggregate following incubation with anti-CD30 antibodies (23). As shown in Fig. 5C, the addition of Ki-1 (3 μg/mL) to Karpas 299 cells led to the formation of large homotypic aggregates. This effect was most likely caused by cross-linking membrane-anchored CD30, as the addition of competitive sCD30 (3,000 units/mL) inhibited aggregate formation. We endeavored to visualize sCD30 bridging on CD153$^+$ cells by means of such homotypic cell aggregation. Ki-1 antibody alone had no influence on the aggregation of the CD30$^-$ cells HMC-1, DG-75, and Reh. However, on CD153$^+$ HMC-1 and DG-75 cells, a strong increase of homotypic aggregate formation was observed when sCD30 was applied in addition to the antibody. As a control, the CD30$^-$/CD153$^-$ cell line Reh was not influenced by sCD30 and antibody. These data strongly suggest that sCD30 also functions as a bridging protein in anti-CD30 antibody binding to CD30$^-$ but CD153$^+$ cells.

To verify the CD153/sCD30/anti-CD30 antibody interaction on the molecular level, we produced a recombinant fusion protein containing the CD153 ectodomain and GST. The protein was coupled to glutathione-coupled Sepharose beads and used in pull-down experiments. Beads were preincubated with purified sCD30

Figure 4. Antibody-stimulated CD30 shedding is catalyzed by ADAM10. *A*, ADAM10-deficient (ADAM$^{-/-}$) human fibroblasts were transfected with human CD30 cDNA. After 36 h, cells were radiolabeled with a mixture of [^{35}S]methionine and [^{35}S]cysteine and stimulated with Ki-1 (3 μg/mL) or PMA (30 ng/mL) in the presence or absence of metalloproteinase inhibitors GI254023X (1 μmol/L) or BB-3644 (1 μmol/L). sCD30 was isolated from cell supernatants by anti-CD30 pull-down and applied to SDS-PAGE. *B* and *C*, ADAM10- and ADAM17-defective cells were transfected with human CD30 cDNA. After 36 h, cells were stimulated with PMA or Ki-1 $\pm$ GI254023X (1 μmol/L) or BB-3644 (1 μmol/L). After 2 h of incubation, sCD30 was determined in the cell supernatants. *Columns*, mean for three independent experiments (U/mL); *bars*, SE.
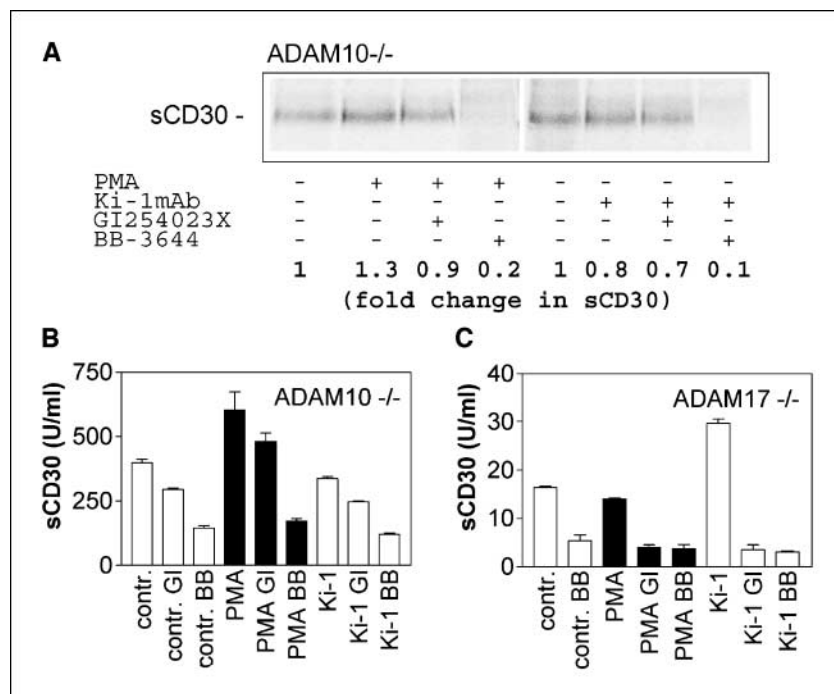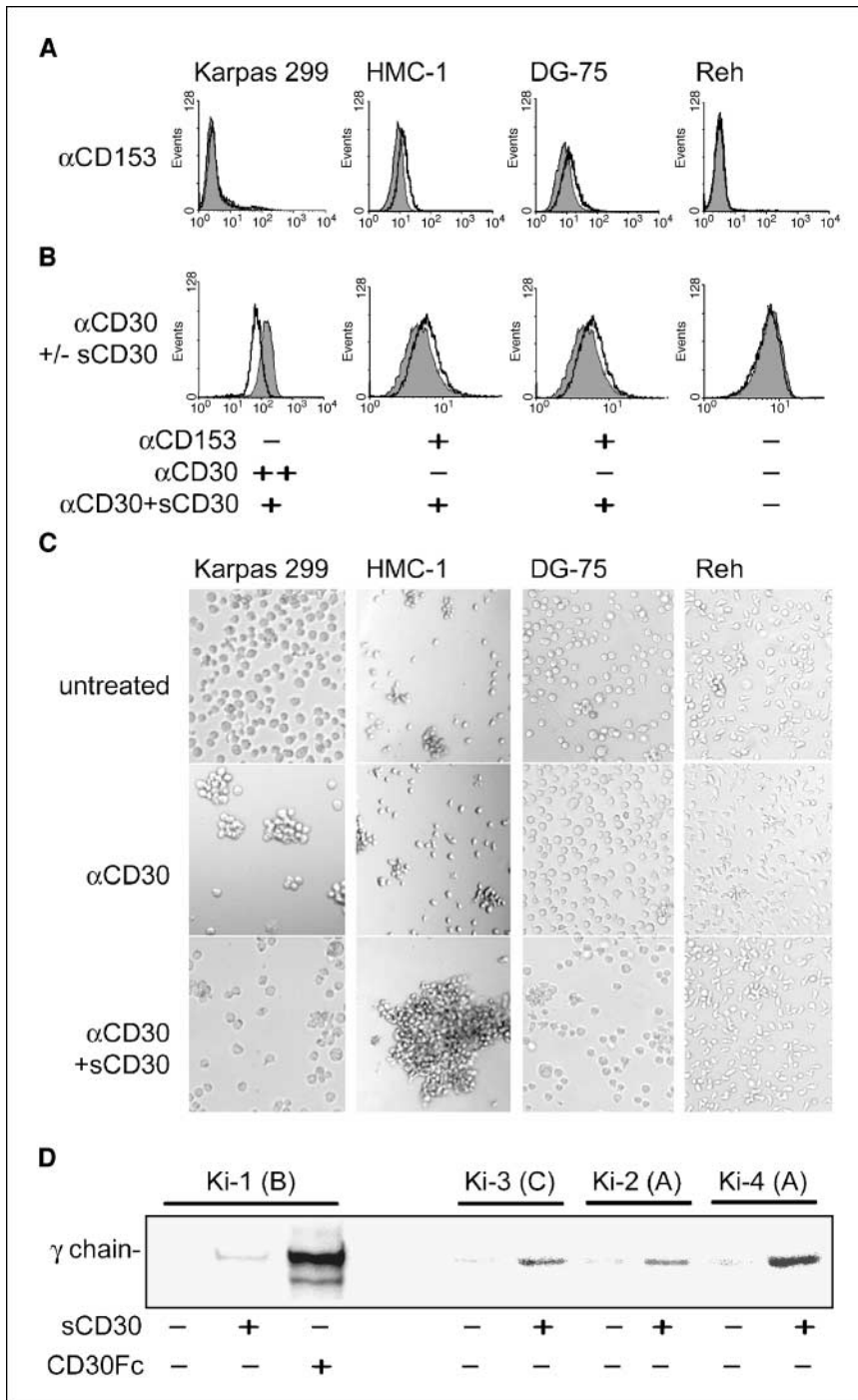
Figure 5. Anti-CD30 antibody binds to CD153 through sCD30 bridging. *A,* CD153 expression. Karpas 299 cells (CD30$^+$/CD153$^-$), DG75 and HMC-1 cells (CD30$^-$/CD153$^+$), and Reh cells (CD30$^-$/CD153$^-$) were incubated with CD153 antibody (*open histogram*) or an isotype-matched control antibody (BH-1, anti-2-phenyloxazolone) and then stained with FITC-labeled goat anti-mouse antiserum. *B,* influence of sCD30 on the binding of Ki-1. Cells were stained using FITC-labeled Ki-1 with purified sCD30 (3,000 units/mL; *open histogram*) or without (*filled histogram*). *C,* detection of homotypic cell aggregation. Cells were incubated alone, with Ki-1 (3 μg/mL), or coincubated with Ki-1 and sCD30 (3,000 units/ml). Cells are shown after 1 h of incubation. *D,* bridging by sCD30. CD153-GST fusion protein, immobilized to GSH-Sepharose, was incubated with [^{125}I]-labeled Ki-1 (cluster B) in the presence or absence of either affinity-purified sCD30 (2,000 units/ml) or CD30Fc (5,000 units/mL). Beads were also incubated with the following anti-CD30 antibodies, [^{125}I]-labeled Ki-2, [^{125}I]-labeled Ki-4 (both cluster A), or [^{125}I]-labeled Ki-3 (cluster C) in the presence or absence of sCD30 (2,000 units/mL). Washed beads were applied to SDS-PAGE. The radioactivity of immunoprecipitated antibody is shown.

(2,000 units/mL), recombinant CD30Fc-fusion protein (5,000 units/mL), or buffer as a control. Washed beads were used to precipitate [^{125}I]-labeled Ki-1 antibody. As shown in Fig. 5*C*, the antibody pull-down is dependent on the presence of sCD30. Both bivalent CD30Fc and monovalent sCD30 were able bind the anti-CD30 antibody and CD153 simultaneously. The Ki-1 antibody, which was used thus far, belongs to the serologic cluster B (13). We also tested cluster A antibodies (Ki-2 and Ki-4) and a cluster C antibody Ki-3. Purified sCD30 enabled the binding of all tested anti-CD30 antibodies to CD153, indicating that antibodies of all clusters are able to target CD30$^-$ but CD153$^+$ cells.

CD153-targeting is inhibited by ADAM10-selective metalloproteinase inhibition. We directly tested the influence of the ADAM10-selective inhibitor GI254023X on the sCD30-dependent mistargeting of a CD153$^+$ mast cell line (HMC-1). The sCD30 release of L540 cells was stimulated with Ki-1 monoclonal antibody (mAb; 3 μg/mL) in the presence or absence of GI254023X (2 μmol/L). The cell-free supernatants were used to stain HMC-1 cells. As shown by flow cytometry, ADAM10-selective shedding inhibition in a coculture experiment strongly reduced the sCD30-dependent Ki-1 binding to the CD30$^-$ mast cell line (Fig. 6).
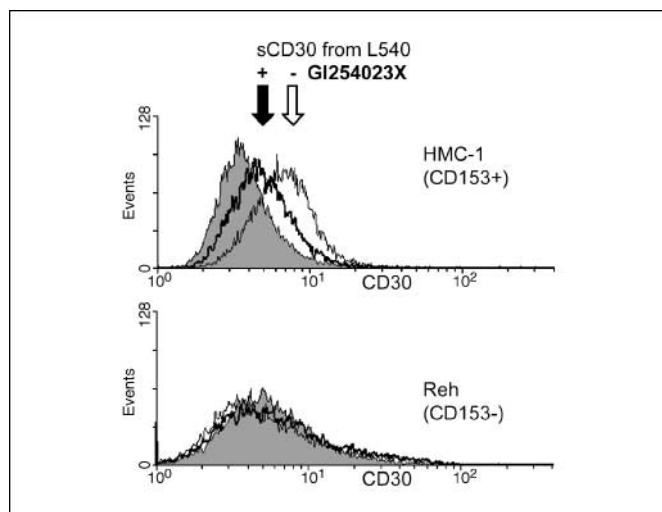
Figure 6. Anti-CD30 antibody binding to mast cells is inhibited by ADAM10-selective metalloproteinase inhibition. L540 cells were treated with Ki-1 (3 μg/mL) for 90 min, in the presence or absence of GI254023X (2 μmol/L). Cell-free supernatants were used to treat HMC-1 cells or Reh cells as a control. Cell-bound antibody was detected using FITC-labeled staphylococcal protein A. Results of a typical experiment.

Discussion

Three major findings emerge from the present study. First, there are at least two different mechanisms that lead to metalloproteinase-dependent CD30 shedding. One is a consequence of PKC activation. This pathway is independent of cytosolic calcium and stimulates the CD30 cleavage through the membrane-anchored disintegrin metalloproteinase ADAM17. A second pathway is stimulated by CD30 ligation; this one is accompanied by an increase of the cytosolic calcium, and we show here for the first time that the CD30 cleavage occurs through the disintegrin metalloproteinase ADAM10. Such antibody-induced shedding generates sCD30/antibody immune complexes. Second, the CD30 ligand (CD153), expressed on many normal cells, is not targeted by anti-CD30 antibodies but instead by sCD30/anti-CD30 antibody immune complexes, rendering antibody-stimulated shedding a significant cause of therapeutic mistargeting. Third, ADAM10 can be selectively inhibited by the metalloproteinase inhibitor GI254023X. This inhibitor blocks antibody-stimulated CD30 shedding and prevents mistargeting but has little effect on most of other metalloproteinase family members (24).

Anti-CD30 antibody binding to CD153 generally demands a bridging protein with distant antibody and ligand binding sites. Franke et al. tested the effect of different monoclonal anti-CD30 antibodies on CD30/CD153 binding (25). Antibodies of three nonoverlapping serologic clusters (clusters A–C) were included. In agreement with our data, they found no inhibition of ligand binding with the cluster B antibody Ki-1. However, in their hands, cluster A and B antibodies showed inhibition of ligand binding, which contrasts our results. A possible explanation is the fact that we used different antibodies [i.e., the original antibodies Ki-2 (A), Ki-3 (C), and Ki-4 (A)]. The latter was tested in clinical phase I studies (4, 26). As the CD30 ligand binding site has not been described thus far, and as antibodies of the same serologic cluster do not necessarily bind the same epitope, it is possible that there are some anti-CD30 antibodies that do not bind to CD153 through sCD30 bridging.

We found two different shedding mechanisms, one of which is activated by PMA, leading to ADAM17-catalyzed CD30 cleavage, and the other activated by CD30 ligation by anti-CD30 antibody, resulting in an ADAM10-catalyzed cleavage. At first glance, the finding that two enzymes account for the ectodomain release of one substrate is striking. However, to date, they are the best-analyzed releasing enzymes, and there is reported redundancy as structurally and functionally diverse proteins, such as CD44, the pro-inflammatory cytokine TNF-α and CX3CL-1, the ligands of the epidermal growth factor receptor, the interleukin-6 (IL-6) receptor, collagen XVII, or Alzheimer's APP, were shown to be ectodomain cleaved by both enzymes (12).

Patients with CD30-expressing Hodgkin's lymphoma or large cell anaplastic lymphoma who were treated with a therapeutic anti-CD30 antibody developed high serum levels of sCD30/anti-CD30 antibody immune complexes (4). Here, we show that immune complexes actively bind to CD153^{+} non-target cells. In contrast to the selective overexpression of CD30 on certain lymphoma cells, CD153 is expressed on many different normal cells of the lymphatic system, such as resting B cells, activated T cells, and mast cells, monocytes, macrophages, granulocytes, and natural killer cells (2, 3). sCD30 binds to CD153 with high affinity (K_D = 4.5 nmol/L; ref. 27) and is functional on CD153-expressing normal cells as it activates neutrophils to release IL-8 for example (28). We therefore speculate that also in the *in vivo* situation, therapeutic anti-CD30 antibodies may bind inappropriately to CD153 on non-target normal cells, through sCD30 bridging. This finding might at least in part explain the dose-limiting cytotoxicity of therapeutic anti-CD30 antibody in clinical studies (4, 26). However, some questions remain to be solved to fully understand the clinical extent of the finding. In particular, it is unknown if CD153^{+} normal cells are equally damaged by all types of attached anti-CD30 mAb/sCD30 immune complexes. Currently, we are investigating whether there are differences between radioimmunoconjugates that, by means of the crossfire effect, damage target cell including adjacent cell and immuno-toxins that require prior internalization.

In our current study, we found that antibody-induced shedding of CD30 is the origin of therapeutic mistargeting. We also showed for the first time that this shedding process was governed by ADAM10-dependent CD30 cleavage. Shedding inhibition is desirable during the course of targeted immunotherapy against shedding-sensitive antigens. As broad-spectrum shedding inhibition in clinical studies was shown to cause substantial side effects, the knowledge of specific metalloproteinases being responsible for individual shedding events might open the possibility for pharmacologic intervention, which may benefit targeted immunotherapy. Exploiting this knowledge, we used an ADAM10-selective shedding inhibitor to block this targeting antibody-induced side effect while keeping other shedding events untouched. We regard this example as a promising approach in target immunotherapy to limit shedding-relevant side effects.

Acknowledgments

References

1. Horie R, Watanabe T. CD30: expression and function in health and disease. Semin Immunol 1998;10:457–70.
2. Younes A, Consoli U, Zhao S, et al. CD30 ligand is expressed on resting normal and malignant human B lymphocytes. Br J Haematol 1996;93:569–71.
3. Molin D, Fischer M, Xiang Z, et al. Mast cells express functional CD30 ligand and are the predominant CD30L-positive cells in Hodgkin's disease. Br J Haematol 2001;114:616–23.
4. Schnell R, Staak O, Borchmann P, et al. A Phase I study with an anti-CD30 ricin A-chain immunotoxin (Ki-4.dgA) in patients with refractory CD30⁺ Hodgkin's and non-Hodgkin's lymphoma. Clin Cancer Res 2002;8:1779–86.
5. Hansen HP, Kisseleva T, Kobarg J, Horn-Lohrens O, Havsteen B, Lemke H. A zinc metalloproteinase is responsible for the release of CD30 on human tumor cell lines. Int J Cancer 1995;63:750–6.
6. Dello SP, Rovida E. Transmodulation of cell surface regulatory molecules via ectodomain shedding. Biol Chem 2002;383:69–83.
7. Hansen HP, Dietrich S, Kisseleva T, et al. CD30 shedding from Karpas 299 lymphoma cells is mediated by TNF-α- converting enzyme. J Immunol 2000;165:6703–9.
8. Black RA. Tumor necrosis factor-α converting enzyme. Int J Biochem Cell Biol 2002;34:1–5.
9. Postina R, Schroeder A, Dewachter I, et al. A disintegrin-metalloproteinase prevents amyloid plaque formation and hippocampal defects in an Alzheimer disease mouse model. J Clin Invest 2004;113:1456–64.
10. Reiss K, Maretzky T, Ludwig A, et al. ADAM10 cleavage of N-cadherin and regulation of cell-cell adhesion and β-catenin nuclear signalling. EMBO J 2005;24:742–52.
11. Maretzky T, Reiss K, Ludwig A, et al. ADAM10 mediates E-cadherin shedding and regulates epithelial cell-cell adhesion, migration, and β-catenin translocation. Proc Natl Acad Sci U S A 2005;102:9182–7.
12. Huovila AP, Turner AJ, Pelto-Huikko M, Karkkainen I, Ortiz RM. Shedding light on ADAM metalloproteinases. Trends Biochem Sci 2005;30:413–22.
13. Horn-Lohrens O, Tiemann M, Lange H, et al. Shedding of the soluble form of CD30 from the Hodgkin-analogous cell line L540 is strongly inhibited by a new CD30-specific antibody (Ki-4). Int J Cancer 1995;60:539–44.
14. Hansen HP, Matthey B, Barth S, et al. Inhibition of metalloproteinases enhances the internalization of anti-CD30 antibody Ki-3 and the cytotoxic activity of Ki-3 immunotoxin. Int J Cancer 2002;98:210–5.
15. Matthey B, Borchmann P, Schnell R, et al. Metalloproteinase inhibition augments antitumor efficacy of the anti-CD30 immunotoxin Ki-3(scFv)-ETA′ against human lymphomas *in vivo*. Int J Cancer 2004;111:568–74.
16. Pavlaki M, Zucker S. Matrix metalloproteinase inhibitors (MMPIs): the beginning of phase I or the termination of phase III clinical trials. Cancer Metastasis Rev 2003;22:177–203.
17. Hansen HP, Recke A, Reineke U, et al. The ectodomain shedding of CD30 is specifically regulated by peptide motifs in its cysteine-rich domains 2 and 5. FASEB J 2004;18:893–5.
18. von Tresckow B, Kallen KJ, von Strandmann EP, et al. Depletion of cellular cholesterol and lipid rafts increases shedding of CD30. J Immunol 2004;172:4324–31.
19. Nagano O, Murakami D, Hartmann D, et al. Cell-matrix interaction via CD44 is independently regulated by different metalloproteinases activated in response to extracellular Ca(2+) influx and PKC activation. J Cell Biol 2004;165:893–902.
20. Hundhausen C, Misztela D, Berkhout TA, et al. The disintegrin-like metalloproteinase ADAM10 is involved in constitutive cleavage of CX3CL1 (fractalkine) and regulates CX3CL1-mediated cell-cell adhesion. Blood 2003;102:1186–95.
21. Hartmann D, de Strooper B, Serneels L, et al. The disintegrin/metalloprotease ADAM 10 is essential for Notch signalling but not for α-secretase activity in fibroblasts. Hum Mol Genet 2002;11:2615–24.
22. Matthews V, Schuster B, Schutze S, et al. Cellular cholesterol depletion triggers shedding of the human interleukin-6 receptor by ADAM10 and ADAM17 (TACE). J Biol Chem 2003;278:38829–39.
23. Bowen MA, Olsen KJ, Cheng L, Avila D, Podack ER. Functional effects of CD30 on a large granular lymphoma cell line, YT. Inhibition of cytotoxicity, regulation of CD28 and IL-2R, and induction of homotypic aggregation. J Immunol 1993;151:5896–906.
24. Ludwig A, Hundhausen C, Lambert MH, et al. Metalloproteinase inhibitors for the disintegrin-like metalloproteinases ADAM10 and ADAM17 that differentially block constitutive and phorbol ester-inducible shedding of cell surface molecules. Comb Chem High Throughput Screen 2005;8:161–71.
25. Franke AC, Jung D, Ellis TM. Characterization of the CD30L binding domain on the human CD30 molecule using anti-CD30 antibodies. Hybridoma 2000;19:43–8.
26. Schnell R, Dietlein M, Staak JO, et al. Treatment of refractory Hodgkin's lymphoma patients with an iodine-131-labeled murine anti-CD30 monoclonal antibody. J Clin Oncol 2005;23:4669–78.
27. Hargreaves PG, Al-Shamkhani A. Soluble CD30 binds to CD153 with high affinity and blocks transmembrane signaling by CD30. Eur J Immunol 2002;32:163–73.
28. Saraiva M, Smith P, Fallon PG, Alcami A. Inhibition of type 1 cytokine-mediated inflammation by a soluble CD30 homologue encoded by ectromelia (mousepox) virus. J Exp Med 2002;196:829–39.

ADAM10 Inhibition of Human CD30 Shedding Increases Specificity of Targeted Immunotherapy *In vitro*

Dennis A. Eichenauer, Vijaya Lakshmi Simhadri, Elke Pogge von Strandmann, et al.

Updated version	Access the most recent version of this article at: http://cancerres.aacrjournals.org/content/67/1/332

Cited articles	This article cites 28 articles, 12 of which you can access for free at: http://cancerres.aacrjournals.org/content/67/1/332.full#ref-list-1
Citing articles	This article has been cited by 6 HighWire-hosted articles. Access the articles at: http://cancerres.aacrjournals.org/content/67/1/332.full#related-urls

E-mail alerts	Sign up to receive free email-alerts related to this article or journal.
Reprints and Subscriptions	To order reprints of this article or to subscribe to the journal, contact the AACR Publications Department at pubs@aacr.org.
Permissions	To request permission to re-use all or part of this article, contact the AACR Publications Department at permissions@aacr.org.